Hindawi
Adsorption Science & Technology
Volume 2022, Article ID 9995335, 14 pages
https://doi.org/10.1155/2022/9995335

Research Article

Adsorptive Detoxification of Congo Red and Brilliant Green Dyes Using Chemically Processed *Brassica Oleracea* Biowaste from Waste Water

Ayesha Kanwal, Rabia Rehman, and Muhammad Imran

Centre for Inorganic Chemistry, School of Chemistry, University of the Punjab, Quaid-e-Azam Campus, Lahore 54590, Pakistan

Correspondence should be addressed to Rabia Rehman; grinorganic@yahoo.com

Received 23 June 2022; Revised 1 September 2022; Accepted 10 September 2022; Published 26 September 2022

Academic Editor: Selvaraju Narayanasamy

Water pollution being a potential risk to mankind is treated in several ways which includes chemical treatments. Among them, adsorption took a prominent position for the removal of many hazardous dyes from waste water. Here in this study, an environment-friendly, inexpensive, and broadly available leaves of *Brassica oleracea* were utilized for adsorption of two carcinogenic dyes, i.e., Congo red and brilliant green. The adsorbent *Brassica oleracea* leaves were collected, dried, and characterized by FTIR and SEM and then utilized in batch manner for dye removal. Isothermal modeling was carried out on data obtained after experiment which show the best fitting of Langmuir with q_{max} 42.553 and 103.093 $mg.g^{-1}$ for Congo red (CR) and brilliant green (BG), respectively. Consequently, a homogenous, monolayer mode of adsorption was followed. Kinetic modeling supported pseudosecond order and Elovich model in most suitable manner. It was also found that a spontaneous, exothermic process provided by the values of thermodynamic parameters (ΔG°, ΔH°, and ΔS°) was calculated.

1. Introduction

Water pollution is one of the major risks for our planet earth. It is established that about 70-80% of water-related issues in emerging countries are associated with industries, which produce tones of colored effluents in their discharge going directly into water bodies [1]. Almost 40000 pigments and dying agents are already found in industrial wastes [2–4]. About 10000 tons per annum of textile dyes are used in industries and along with printing industry, it makes 10-15% of total dying agents released in water bodies [3, 5, 6]. All these effluents coming out of industries cause severe damage to the ecosystem especially in these water bodies. Whenever this polluted water is consumed by humans for daily shore, it causes life-threatening damage towards human health as it is responsible for high mutation index and results into different kinds of cancers [4, 5].

Previous literature revealed many hazardous effects of water containing dyes like brilliant green and Congo red which includes cancers of different types, skin diseases, gastrointestinal poisoning, and also issues related to respiratory system in humans [6, 7]. Minor concentration of such dyes in water cannot be overlooked because even 0.005 ppm of such dyes in water can interfere in light path which results into inefficient photosynthesis by the aquatic plants and rest of the ecosystem suffers as a result. Hence, the dye removal is a must before throwing all the effluents directly into water bodies [8].

Various in-practice traditional methods that include photochemical, biological, and chemical treatments [9–11] are in practice for the removal of such effluents, such as ozonation [12], coagulation [13], fungal decolorization [14–16], adsorption, flocculation, and electrochemical technique [17, 18]. All these techniques are efficient in one way or the other but are complicated and problematic towards various environmental aspects being expensive and produce several hazardous by-products [19, 20]. So, adsorption techniques emerged as the most suitable method among all these in response to its availability (of adsorbent), efficiency, and cost effectiveness. A number of different adsorbents have been

used both as raw as well as chemically modified for the removal of dyes, i.e., brilliant green and Congo red (Figure 1).

Brassica oleracea commonly known as cauliflower is an annual plant which belongs to family Brassicaceae. It grows in sunny and moist climate in temperature range of 21-29°C [21]. In recent years, 25.5 million tons of *Brassica oleracea* was produced globally. 92% of it is composed of water and carbohydrates along with some essential vitamins. Apart from all this, it contains number of nonnutrient phytochemicals and dietary fibers [22]. From decades, brassica is a part of major cuisines of the world but mostly its stalk and leaves are not used in cooking that goes directly into waste. It is also reported as anticancerous in nature by different researchers [23–25]. Current study *Brassica oleracea* is picked for adsorption of selected dyes, and its adsorption efficiency is studies under appropriate operation conditions.

2. Experimentation

2.1. Chemicals. All the chemicals as well as apparatus used were of analytical grades which include brilliant green dye (λ_{max} = 625 nm), Congo red (λ_{max} = 498 nm), HCl (11.6 M), NaOH (Mol. Wt. 40 g), and distilled water, and all of these were obtained from Sigma-Aldrich. Vis-spectrophotometer Electric Balance ER-120A, Electric grinder (Ken-Wood), pH meter (HANNA pH 211), and Electric shaker 721 were also used for this study.

2.2. Preparation Characterization of Biosorbent. The biosorbent *Brassica oleracea* is nontoxic and is available easily almost all parts of Punjab, Pakistan. The sample used in this particular study was acquired from the rural areas of Layyah district, Punjab. After collecting the leaves of *Brassica oleracea* (BO) ,it was thoroughly washed with tap water to remove all the dust trapped. Later on, it was trimmed and washed again with distilled water; then, the material was sundried for 8-10 days. This again was placed in oven at 80°C for 3 days to get rid of all the remaining moisture present in it. This dried sorbent material was then ground and sieved to 60-70 mesh size, and a fine powder was obtain [26]. To eliminate any remaining moisture, it was oven dried once again and then poured into air tight plastic jars to use it further. It is summarized in Figure 2.

2.3. Synthetic Waste Water Preparation. 1000 ppm solutions of both brilliant green (BG) and Congo red (CR) dyes were prepared by adding 1 g per 1000 mL of distilled water in a measuring flask. All other solutions of dyes for further use were prepared by diluting this stock solution of 1000 ppm. For optimization of the parameters to determine the adsorption capacity of BO against dyes, 25 mL of each dye was taken in 100 mL flasks, and operational conditions were finalized.

2.4. Optimization of Operational Conditions. Various operational conditions were optimized to get better results in a batch adsorption technique. These operational parameters include the following: adsorbent dose (range 0.2-2 g with variation 0.2 g), pH (range 1-10), temperature (range 20-70°C), contact time (range 5-60 min), and agitation rate

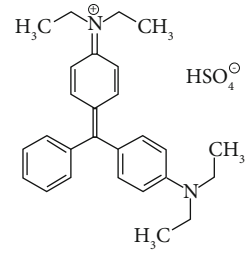

Brilliant Green

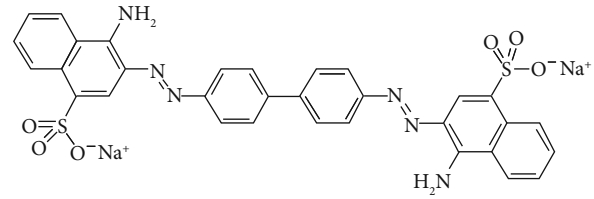

Congo Red

Figure 1: Structural formulas of brilliant green (BG) and Congo red (CR).

(range 40-240 rpm difference 40 rpm). To check the reliability of the adsorption results, isothermal and kinetic modeling was done for both the dyes. Following formulas were utilized to determine the % adsorption as well as amount of dye adsorbed for each dye.

$$\%\text{Adsorption} = \left(\frac{C_o - C_e}{C_o}\right) \times 100, \qquad Q = \left[\frac{(C_o - C_e)V}{W}\right]. \tag{1}$$

Here, Q is the amount of dyes (mg/g), C_o is the initial concentration (ppm), C_e represents equilibrium concentration of BG and CR, V represents volume (L), and W shows weight (g).

3. Results and Discussions

3.1. Characterization of Adsorbent. FTIR spectrum of *Brassica oleracea* leaves presented here shows a number of major functional groups present that it is responsible for the binding of dye onto the adsorbent (Figure 3). Here, the band at 3855 cm^{-1} and 3738 cm^{-1} indicates the presence of OH group along with carboxylic moieties at 3297 cm^{-1} while the bands at 2917 cm^{-1} and 2849 cm^{-1} show the presence of C–H functional moieties. The bands present at 1653 cm^{-1} and 1510 cm^{-1} indicate N-H stretching. Graph also shows a band at 1420 cm^{-1} which shows carboxylic bending frequency. Figure 3 presents the FTIR spectra of adsorbent BO before and after dye loading, BO, BO-CR, and BO-BG, respectively. Here, the shift in the region of 3855 and 3738 cm^{-1} to 3881 cm^{-1} (for CR) and 3898 cm^{-1} (for BG) depicts the involvement of OH bond because of hydrogen bonding between the molecules of adsorbent and dyes. Also, a clear

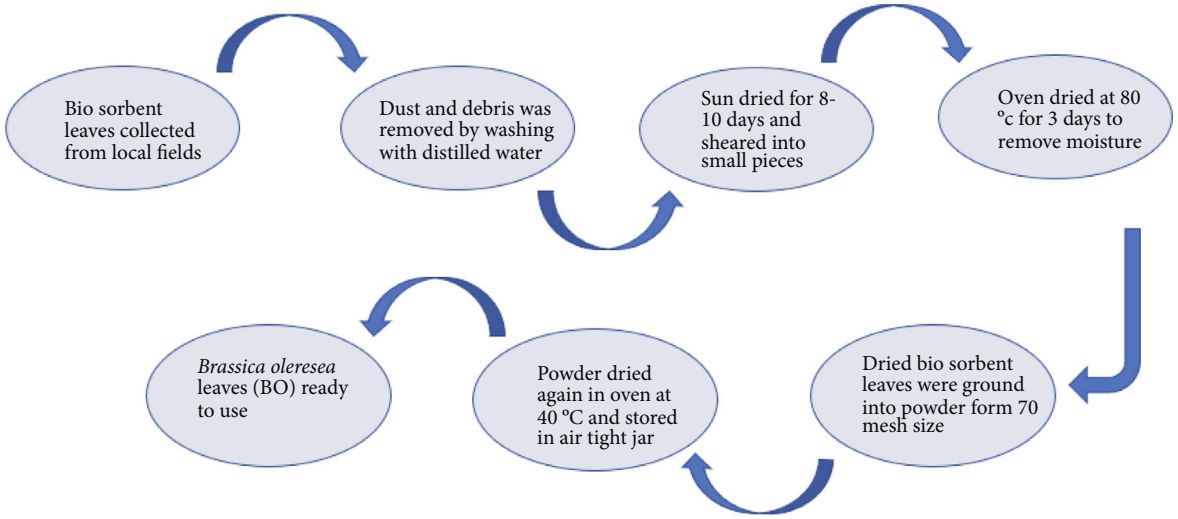

Figure 2: Schematic representation of the steps involving preparation of adsorbent. The biosorbent BO was characterized using various useful techniques, i.e., Boehm titration (to determine acidic and basic moieties) pH, and other physioanalytical data Table 1 [27]. FTIR and SEM were also carried to get further understanding of the sorbent behavior.

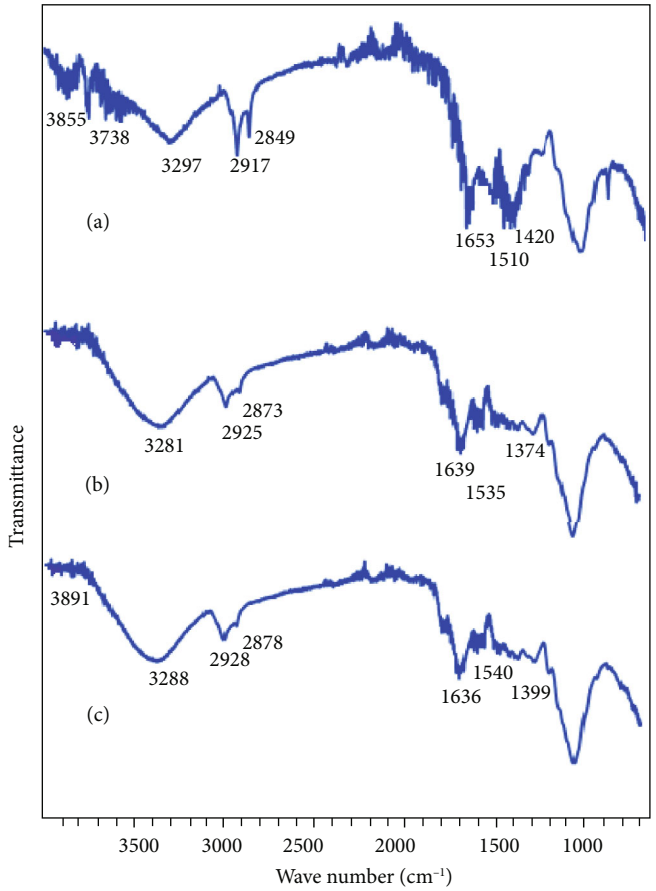

Figure 3: FTIR spectra of (a) *Brassica oleracea* (BO), (b) Congo red loaded *Brassica oleracea* (BO-CR), and (c) brilliant green loaded *Brassica oleracea* (BO-BG).

change in wavenumber at carboxylic region from 3297 to 3281 cm^{-1} (Figure 3(b)) and 3288 cm^{-1} (Figure 3(c)) advocates the involvement of OH from carboxylic moiety. N-H stretching region shifts to 1639 and 1535 cm^{-1} in BO-CR and to 1636 and 1540 cm^{-1} in BO-BG spectrum, respectively. A hypsochromic shift in COOH bending peaks was also

observed for CR 1374 cm^{-1} and for BG 1399 cm^{-1}. These shifts in major functional moieties accompanied by oxygen containing groups advocate a clear interaction between adsorbent and dye molecules, as the involvement of such functional groups promotes adsorption of dyes on adsorbents [28].

The data given in Table 1: the presence of small amount of moisture, volatile matter, and ash content indicates little particle density that favors adsorption over this particular biosorbent [29]. Porosity, i.e., number of pores per unit area, depicts good adsorption capacity. It is described that in case of some cationic dye adsorption occurs spontaneously due to presence of electrostatic interaction along with hydrogen bonding between the dye (cationic) and the adsorbent while for anionic dye adsorption hydrogen bonding play vital role [30].

SEM image of the adsorbent BO shown in Figure 4 represents the presence of rough and porous surface which always play effectively towards the adsorption of dye on to the adsorbent surface. More porous adsorbent surface have large physiosorption tendency to adsorb more dye molecules [31].

3.2. Operational Condition Optimization. pH_{pzc} (point of zero charge) was measured for *Brassica oleracea* (BO) which turned out to be 8 that provides a strong basic medium for the adsorption of dyes. pH_{pzc} actually helps in determining the sensitivity towards linear range of pH. It also reveals the surface-active centers and adsorption capacity of that adsorbent surface [30]. Literature has widely reported about the pH_{pzc} of agriwaste by a number of researchers. Cationic dyes get more adsorption if $pH > pH_{pzc}$, i.e., negative charge increases while anionic dyes get favorable adsorption condition if $pH < pH_{pzc}$, i.e., positive surface charge increases [32, 33] (Figure 5(a)).

Optimum time of contact of BO for both the cases, i.e., CR and BG shown in Figure 5(b) which depicts optimum time for CR and BG is 30 and 40 minutes, respectively. Both the trends present a gradual increase in % age adsorption until their optimums were reached, and a downward trend started over there. Optimum adsorbent dose of BO for CR and BG was turned out to be 1 and 1.4 g, correspondingly. Figure 5(c) shows an increasing trend initially, and then the values of % age adsorptions decreased for both of the dyes. Values obtained from the procedure for optimum pH of *Brassica oleracea* present 1 and 7 pH for CR and BG, respectively (Figure 5(d)). Literature shows that Congo red (CR) is more likely to be adsorbed at acidic pH because of its anionic nature and interacts with adsorbent surface with electrostatic interaction [34]. This electrostatic interaction between the two decreases as the pH of the system gets more basic. It occurs because of the increase in negatively charged particles in the solution and attraction converts into electrostatic repulsion [35, 36]. On the other hand, BG acts as cationic dye and as literature states that cationic dyes show spontaneous adsorption because of growing number of positively charged particles. Hence, there occurs strong hydrogen bonding along with electrostatic attraction [37, 38].

Table 1: Physioanalytical data of *Brassica oleracea* (BO).

Parameters		BO values
Bulk density ($g.mL^{-1}$)		0.505
Dry density ($g.mL^{-1}$)		0.478
Porosity (%)		0.83
Moisture		3
Ash		99.7
Volatile matter		0.3
Carboxylic acid		1.98
Phenols		0.28
Lactones		0.01
Basic sites		1.93
pH_{pzc}		8
Elemental content ($mg.Kg^{-1}$)	C	54.81%
	O	38.89%
	Na	1.75%
	Ca	4.55%

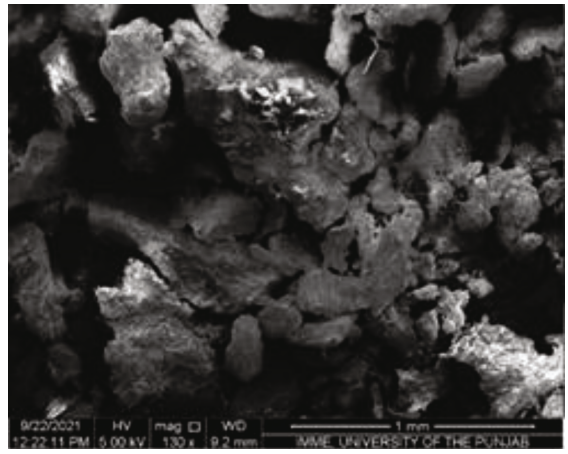

Figure 4: SEM image of BO.

Agitation speed of BO for the removal of CR and BG was found to be 120 rpm and 100 rpm, respectively. Shaking speed of solution-containing adsorbent is related to the interaction of molecules between dye, and speeds higher than mentioned above were not suitable for this particular case as there occurs a clear decline in % age adsorption of dyes (Figure 5(e)).

Temperature optimization was also done for BO for both CR and BG dyes that turned out to be 40°C and 50°C. The higher temperature of the solution higher will be the diffusion rate of dye at the adsorbent surface that results into increased adsorption of the dye but as temperature increased over the optimum, a clear decline in the % age adsorption was observed. This decline is related to very high movements of molecules that reverses the adsorption process [10] indicated in Figure 5(f).

3.3. Adsorption Isothermal Studies. The relationship established between the adsorbate and adsorbent is determined

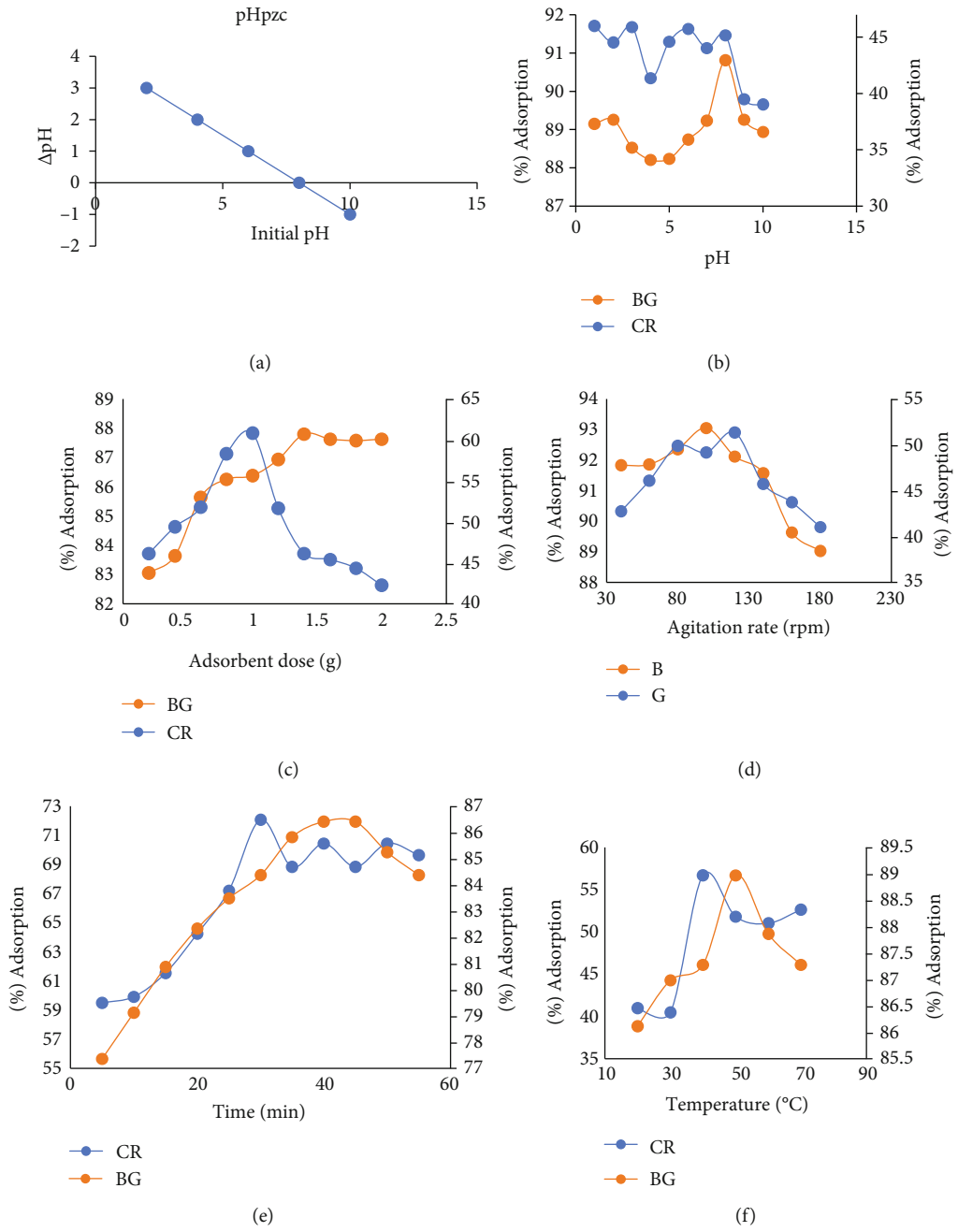

Figure 5: Adsorption parameter for Congo red (CR) (% age adsorption y- axis on the right hand side) and brilliant green (BG) (% age adsorption y-axis on the left hand side) adsorption on Brassica oleresea (BO): (a) pHpzc, (b) contact time, (c) adsorbent dose, (d) pH influence, (e) agitation rate, and (f) temperature change.

by isothermal modeling. It also assessed the authenticity and mechanism of the experiment performed [39]. Following isothermal models were applied to get all this information, i.e., Langmuir, Freundlich, Temkin, and the Dubinin–Radushkevich isotherms.

3.3.1. Langmuir Isotherm. It conveys about the relation between equilibrium concentration and the amount of adsorbate per unit weight of sorbent. Langmuir isotherm established on the idea that adsorption occurs as monolayer on homogenous surface of adsorbent [40]. Langmuir isothermal model (linear) given in Eq. (2) is as follows:

$$\frac{1}{q_e} = \frac{1}{bq_{\max}} \bullet \frac{1}{C_e} + \frac{1}{q_{\max}}, \tag{2}$$

where *Ce* represents equilibrium concentration (mg/L) of BG and CR dyes, *qmax* is the maximum sorption capacity (monolayer) of sorbent, q_e is the quantity of dye adsorbed

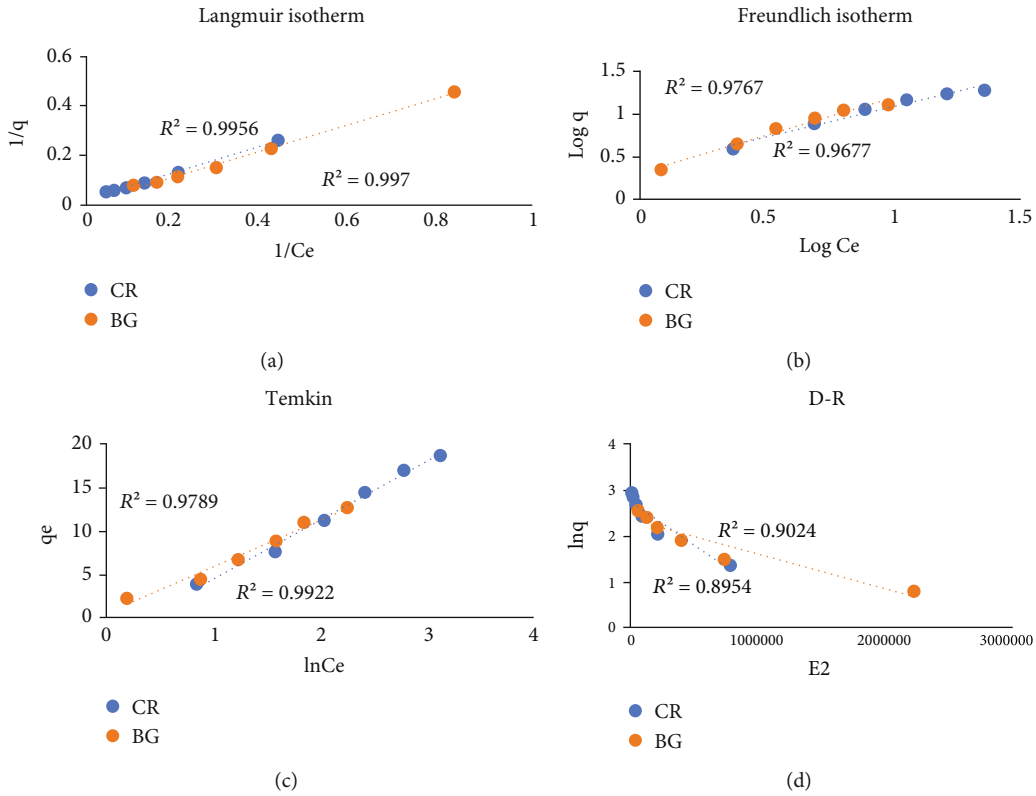

FIGURE 6: Adsorption isotherms. A comparative plot of CR and BG for adsorption on *Brassica oleracea* BO. (a) Langmuir isotherm, (b) Freundlich isotherm, (c) Temkin isotherm, and (d) Dubini-Radushkevich isotherm.

(mg/g), and b is the sorption ability of the adsorbent. R_L also known as separation factor is a dimensionless quantity which presents the probability of sorption. It is calculated by the equation (3):

$$R_L = \frac{1}{1 + K_L C_o}, \tag{3}$$

where C_o is the initial concentration of dyes, and K_L represents Langmuir constant (L/mg).

R_L values of CR and BR dyes for the adsorption on BO are found to be 0.2789 and 0.4794 both the values are in between 0 and 1 that illustrates the feasibility or favorable condition for adsorption of dyes (Figure 6). Literature has given following cases for the value of R_L: $0 < R_L < 1$ means the promising adsorption results, $R_L > 1$ means not favorable, $R_L = 1$ or $R_L = 0$ means linear adsorption, and if $R_L <$ 0, it will be irreversible [41]. The value of R_L for both the dyes mentioned above clearly shows effectual use of the Langmuir isothermal model. q_{max} is the maximum adsorption capacity for both the dyes CR and BR which are 42.55 and 103.09 $mg.g^{-1}$ which indicated that the adsorption of BG dye is more favored on BO biosorbent rather than for CR (Table 2, Figure 6(a)), compared with literature in Table 3. It shows monolayer of dye gets adsorbed homogenously on the binding sites distributed over the surface of the adsorbent BO [42].

3.3.2. Freundlich Isotherm. It is employed to determine multilayer, on-ideal heterogeneous adsorption pattern. This isotherm supports the idea of reversible adsorption on a rough adsorbent surface [43]. Equation Eq. (4) shows the linear for of Freundlich isothermal model

$$\log q_e = \log K_F + \frac{1}{n} \log C_e, \tag{4}$$

where K_F is known as Freundlich constant and represents biosorption ability, n is known to be frequency or strength of biosorption, and $1/n$ is actually related to heterogeneity of the adsorbent surface [44, 45]. The graph plotted between log q_e vs. log C_e gave straight lines and by using intercept and slope of the graph values of n and K_F which can be determined. The data given in Table 2 shows that the values of n for both the dyes CR and BG are found to be 1.419 and 1.138, correspondingly, which signify a good adsorption happened as $1 < n < 2$ depicts good adsorption. Also, R^2 happened to be higher in Langmuir's case rather than for Freundlich that favors the previous one (Figure 6(b)).

3.3.3. Temkin Isotherm. It validates the relative decrease of sorption energy. It says heat of adsorption ($\Delta Hads$) of adsorbent used, decline in linear fashion as the surface coverage of adsorbent increases [46]. Temkin isotherm advocates the veiled interaction among adsorbate and adsorbent. The linear equation (5) is given below:

Table 2: A summary of adsorption isothermal data of Congo red (CR) and brilliant green (BG) dyes adsorbed on *Brassica oleracea* (BO).

Isotherm model	CR	BG
Langmuir		
Q_m (mg.g^{-1})	42.55	103.09
R_L (L.mg^{-1})	0.27	0.47
b (L.g^{-1})	0.04	0.01
R^2	0.99	0.99
RMSE	1.07	1.06
Freundlich		
n	1.41	1.13
$1/n$	0.70	0.88
K_f (mg.g^{-1})	2.37	2.02
R^2	0.97	0.97
RMSE	1.38	0.95
Temkin		
B (J.mol^{-1})	6.77	5.32
A (L.mg^{-1})	0.70	1.09
R^2	0.99	0.98
RMSE	1.86	0.52
D - R		
Q_m (mg.g^{-1})	18.17	13.03
B_D (mol^2. (KJ^2)$^{-1}$)	0.000004	0.000002
E_D (KJ.mol^{-1})	0.35	0.5
R^2	0.96	0.98
RMSE	2.10	1.2

$$q_e = B_T \ln C_e + B_T \ln A_T, \tag{5}$$

where A_T is equilibrium binding constant (L/g), and B_T represents Temkin isotherm constant (J/mol). This B_T depicts that which type of interaction prevails between sorbent and dyes, i.e., physical or chemical. $B_T < 8$ favors physical association while $B_T > 8$ supports chemical connotation [47–49]. Data presented in Table 2 shows B_T values for CR and BG, 6.778, and 5.323, respectively; both for CR and BG, B_T values are below 8 which advocates the weak physical connotation between the sorbent BO and both the dyes CR and BG. Figure 6(c) shows graph between lnCe and q_e. The values of R^2 for the Temkin model are found to be less than Langmuir which depicts poor fitting of this model compared to that of Langmuir model.

3.3.4. Dubinin–Radushkevich Isothermal Model. It is considered to be relatively broader than Langmuir and Freundlich isotherms. It contributes in determining adsorption energy and distinctive absorbency mechanism [50]. The equation given illustrates the biosorption of gases on adsorbents (especially microporous). This model supports the multilayer adsorption supported by Vander Waal's forces [51]. Linear form *D-R* equation is (6) given below:

$$\ln q_e = \ln q_n - B_D \varepsilon^2, \tag{6}$$

$$\varepsilon = \mathrm{RT} \ln\left(1 + \frac{1}{C_e}\right). \tag{7}$$

q_e represents amount of CR and BG adsorbed, C_e presents equilibrium concentration, q_m (mg/g) is known as *D-R* constant responsible degree of adsorption, ad B_D (mol^2 · kJ^{-2}) is free energy and ε named as Polanyi potential. The mean free energy E (kJ.mol^{-1}) can be calculated by eq. (8):

$$E = \frac{1}{\sqrt{2B}}. \tag{8}$$

E is helpful for the interpretation of mechanism of adsorption, and its value determines the type of adsorption carried out, i.e., $E < 8$ inclined to physiosorption, and $8 < E < 16$ presents ion exchange process while $E > 16$ favors chemisorption sort of adsorption [52]. The data staged in the table gives E visible less than 8 that eventually favors the physiosorption mechanism. E (mean free energy) for CR and BG is 0.35 and 0.5 (kJ.mol^{-1}), correspondingly.

All the adsorption isotherms applied, Langmuir, Freundlich, Temkin, and Dubinin-Radushkevish, and regression factor R^2 is found be the highest for Langmuir isotherm that is why it is more likely to be followed.

3.4. Kinetic Studies. Biosorption rate of reaction was studied by applying the standard kinetic models which include Elovich, Lagergren pseudofirst order model, and Ho's pseudosecond order model. To get the best fittin,g among them, percent relative deviation was measured by eq. (9):

$$P(\%) = \frac{100}{N}\left\{\frac{q_{e(\exp)} - q_{e(\mathrm{cal})}}{q_{e(\exp)}}\right\}, \tag{9}$$

where $q_e(\exp)$ is the experimental sorption ability (mg.g^{-1}), $q_e(\mathrm{cal})$ represents calculated value of sorption ability; it is obtained by using kinetic models, and N shows no. of observations [69].

3.4.1. Elovich Model. It favors multiple coating of dye as it is based on the idea of exponential increase in adsorption, powered by the rise of sorption locations on adsorbent [70]. This model was first applied in favor of chemisorption process of gases [65]. Linear equation of the Elovich model is shown in eq. (10) [71]:

$$q_t = \frac{\ln(a \times b)}{b} + \frac{lnt}{b}, \tag{10}$$

where q_t (mg.g^{-1}) is the amount of dye carried by adsorbent at any time t, a (g.mg^{-1}) shows rate of adsorption in the start of process, and b (g.mg^{-1}) presents the total no. of adsorption spots occupied by dye molecules. Higher the value of a, more it will support chemisorption. For this model, a plot of lnt vs. q_t gives the values of Elovich constants using slope and intercept (Figure 7(a)).

Table 3: Previously announced comparative adsorption capacity (q_{max}) data.

Biosorbents	Adsorption capacity (q_{max}) (mg.g^{-1})	References
Decoloration of Congo red dye		
Coir pith activated carbon	6.72	[53]
Cattail root	38.9	[54]
Rice husk	3.08	[55]
Banana peel	18.2	[56]
Orange peel	14	[56]
Cationic surfactant modified tea waste	106.4	[57]
Jute stick powder	35.7	[58]
Bael shell carbon	98.03	[59]
Bamboo dust carbon	101.9	[60]
Desiccated coconut waste	48.8	[61]
Vernonia amygdalina leaf powder	57.4	[62]
Brassica oleracea leaf powder	42.55	[this study]
Decoloration of brilliant green		
Rice husk ash	26.18	[20]
Watermelon peel	25	[63]
Pomegranate peels nanoparticle	24.57	[64]
Areca nut husk	18.21	[41]
Date pit activated carbon	77.8	[7]
Trapa natans peel citric acid treated	128	[65]
Citrullus lanatus peel citric acid treated	189	[65]
Citrullus colocynthis tartaric acid treated	79.36	[66]
Cashew nut shell activated carbon	243.9	[67]
Soybean straw-derived biochar	83.33	[68]
Trapa natan	50.51	[34]
Brassica oleracea leaf powder	103.09	[this study]

3.4.2. Pseudofirst Order Model. It is also known as the Lagergren model which is recognized on the postulate that adsorption is comparable to the number of attaching sites for the dye on the adsorbent surfaces [72].

$$\ln (q_e - q_t) = \ln q_e - k_1 t, \tag{11}$$

where k_1 (h^{-1}) represents as rate constant, and q_t and q_e show amount of dye adsorbed at any moment of time t and at equilibrium, respectively. If the values of q_e and q_t have more difference (P), then this model becomes futile. Also, the -ive sign with value of P depicts that adsorption rate at equilibrium is more than any other time t along with this value of regression factor R^2 which is also responsible to decide either this model is effective or not. Here, R^2 value is quite less than 1; so, this model does not fit on adsorption data (Table 3, Figure 7(b)).

3.4.3. Pseudosecond Order Model. Ho's model is based on the statement that reaction rate of adsorption process is related to concentration of dye and square of attaching sites for dye on adsorbent surface [73, 74]. Following equation presents linear form of this model:

$$\frac{t}{q} = \frac{1}{k_2 q_{e^2}} + \frac{t}{q_e}, \tag{12}$$

where k_2 shows the rate constant for Ho's model, and q_e and q_t depict adsorption ability at equilibrium and any time interval, correspondingly.

Here, the lesser difference between q_e (exp) and q_e (cal) approves the chemisorption type of adsorption; also, the value of P (%) is low along with higher correlation coefficient (R^2) [75]. The values of R^2 for CR and BR are found to be 0.994 and 0.996, correspondingly. The value is closer to unity which depicts that pseudosecond order is more likely to be followed (Table 4, Figure 7(c)).

3.5. Adsorption Mechanism. To determine the mechanism followed by adsorption process, two different models were applied, i.e., intraparticle diffusion model and film diffusion model [76, 77].

Intraparticle diffusion or Weber Morris model is presented as

$$q_t = k_{ip} t^{1/2} + C. \tag{13}$$

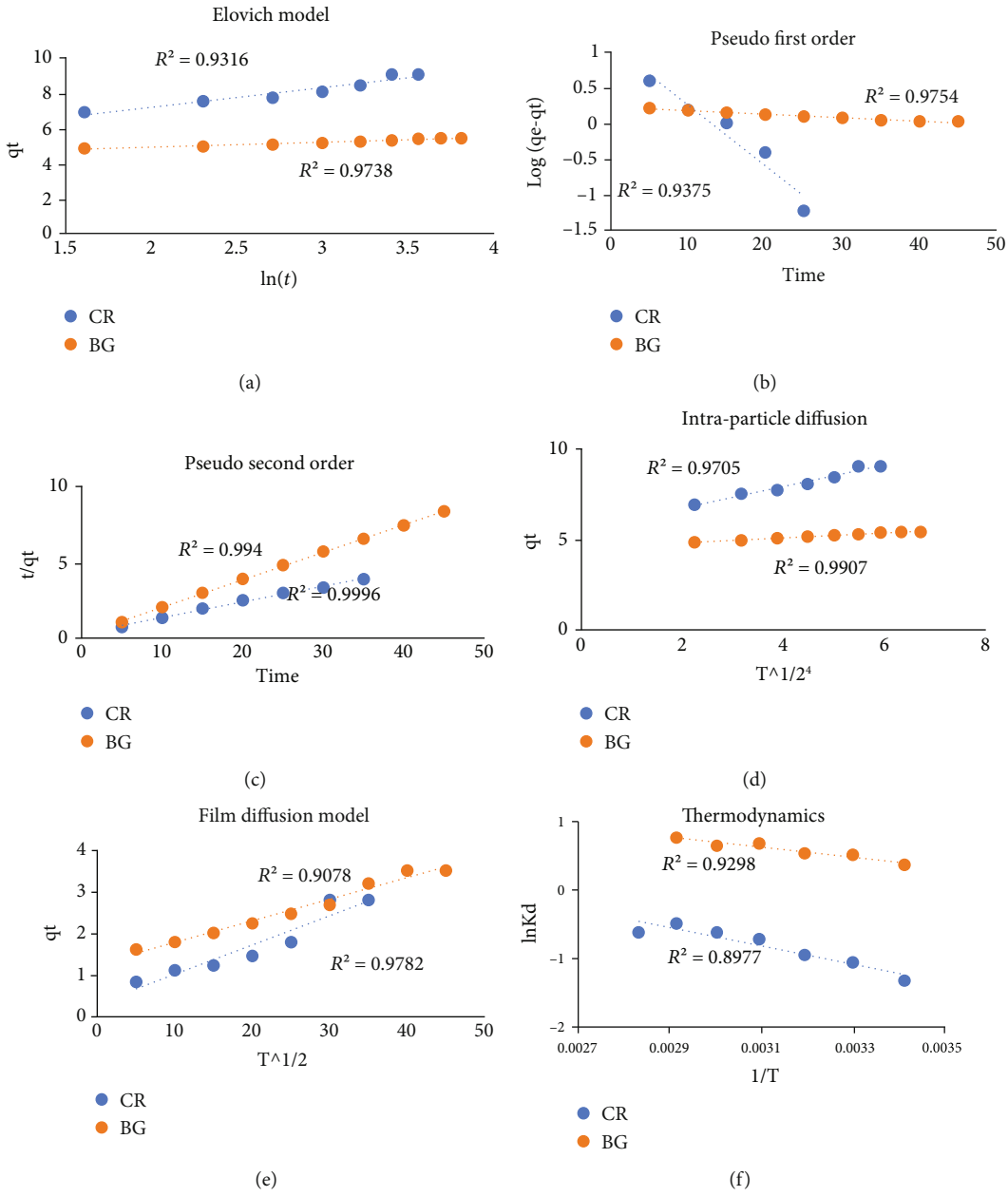

FIGURE 7: Comparative kinetic and thermodynamic studies plots for CR and BG dye removal by BO. (a) Elovich plot, (b) pseudofirst order, (c) pseudosecond order, (d) intraparticle diffusion model, (e) film diffusion model, and (f) thermodynamic parameters of CR and BG dyes.

K_{ip} is known as coefficient of intraparticle diffusion, and C is called boundary layer influence.

The plot (q_t vs. $t^{1/2}$) presenting straight line crossing the origin is clearly suggesting the intraparticle diffusion mechanism if not then film diffusion mechanism or Boyd's mechanism will be followed (Figures 7(e) and 7(f)).

Boyd's model is built on partially attained equilibrium related to variable time as given below [78],

$$F = 1 - \frac{6}{(3.1416)^2} \exp(-B_b t),$$
$$B_b = -0.4997 - \ln\left(1 - \frac{q_t}{q_e}\right), \quad (14)$$

where B_b is Boyd's constant while F represents partially attained equilibrium (q_t/q_e).

R^2 compared given in Table 3 for both CR and BG shows that intraparticle diffusion mechanism was followed.

3.6. Thermodynamic Studies. The variation in temperature of the adsorption system visibly affects the kinetic energy of the dyes, CR and BG. This factor speeds up rate of diffusion as the interaction of dye molecules occurs with porous and spongy surface. Certain operational parameters of thermodynamics, i.e., Gibbs free energy ΔG°, change in entropy (ΔS°), and change in enthalpy (ΔH°) were utilized to determine the efficiency and adsorption rate of dyes CR and BG using Figure 7(f). Table 5 presents the values of ΔG°, ΔH°,

Table 4: A brief summary of kinetic parameters applied on adsorption of dyes on BO.

Kinetic model	CR	BG
Elovich		
a (g.mg^{-1}.min^{-1})	0.89	3.58
b (g/mg)	94.16	1533663.33
$R2$	0.931	0.93
RMSE	0.078	0.076
Pseudofirst order		
q_e (exp) (mg.g^{-1})	9.36	4.835
q_e (calc) (mg.g^{-1})	3.00	1.2482
K_1 (min^{-1})	-0.0021	-0.0001225
R^2	0.93	0.97
P (%)	8.49	8.14
RMSE	2.87	2.27
Pseudosecond order		
K_2 (g.mg^{-1} min^{-1})	29.23	6.64
q_e (calc) (mg.g^{-1})	9.66	5.52
q_e (exp) (mg.g^{-1})	9.36	5.5
$t^{1/2}$	0.00354	0.03
h (mg.g^{-1}.Min^{-1})	2728.48	203.1
R^2	0.99	0.99
P (%)	-0.4	-0.05
RMSE	0.24	0.16
Intraparticle diffusion		
k_{id} (mg.g^{-1}.Min$^{-1/2}$)	0.6	4.53
C (mg·g^{-1})	5.52	0.14
R^2	0.97	0.99
Film diffusion		
K_{fd} (1/min^{-1})	0.09	0.01
R^2	0.94	0.97

Table 5: Thermodynamic parameters of dyes removal by **BO**.

Adsorbate	Temp (K)	$K_D = q_e/C_e$	ΔG° (kJ/Mol)	ΔH° (kJ/mol)	ΔS° (J/mol K)
CR	293.16	0.27	3.21	-13.66	35.94
	303.16	0.35	2.67		
	313.16	0.39	2.46		
	323.16	0.488	1.92		
	333.16	0.54	1.72		
	343.16	0.61	1.39		
	353.16	0.54	1.82		
BG	293.16	1.44	-0.89	-6.13	24.19
	303.16	1.67	-1.29		
	313.16	1.71	-1.40		
	323.16	1.97	-1.82		
	333.16	1.91	-2.01		
	343.16	2.15	-2.72		

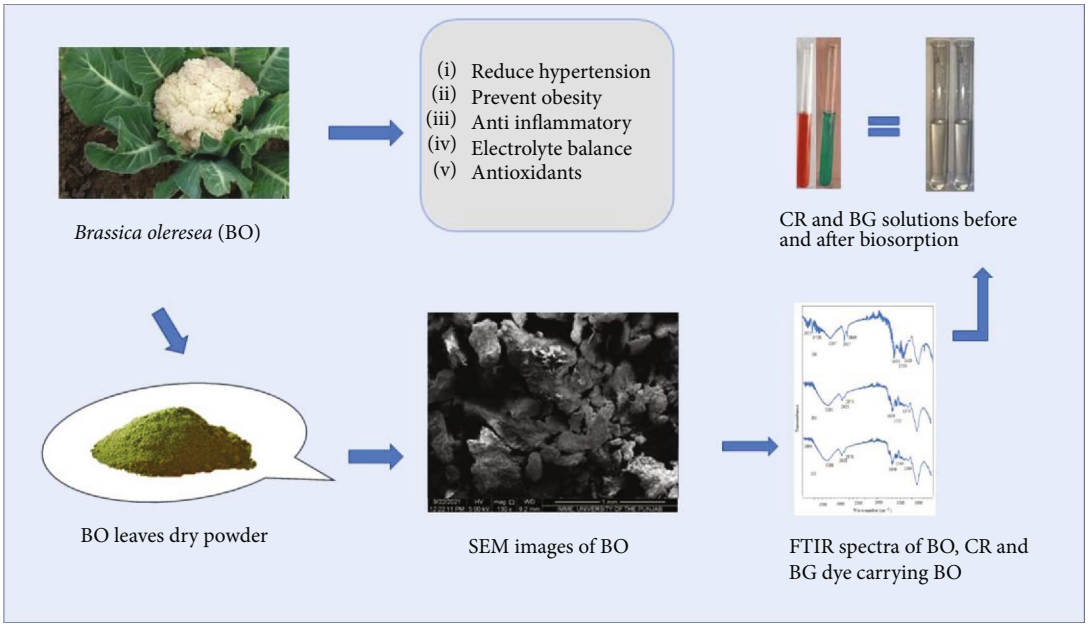

Figure 8: Summarizing whole work in one frame.

and ΔS°, and -ive value of free energy and enthalpy of the system supports spontaneous and exothermic nature of reaction while +ive entropy of the system defends the randomness of adsorbent surface [76, 79, 80]. These were calculated by equation below:

$$\Delta G^{0} = \{RT(\ln K_{D})\}, \tag{15}$$

where R is known as general gas constant, T (K) is the temperature, and K_D is the distribution coefficient.

$$K_{D} = \frac{C_{e}}{q_{e}}. \tag{16}$$

The value of ΔH° ranging 2.1 to 20.9 kJ/mol is an emphasis on physiosorption while its value between 80 and 200 kJ/mol is due to stronger interface resulting chemisorption. A linear plot $1/T$ vs. ln K_D presented in the figure which give the values of ΔG°, ΔH°, and ΔS°, using the following equation:

$$\Delta G^{\circ} = \Delta H^{\circ} - T\Delta S^{\circ}. \tag{17}$$

Here, the value of G is found to be negative along with H (negative), and S is found to be positive; all these factors show a spontaneous, exothermic adsorption reaction with positive entropy or randomness of the adsorption system [81].

4. Conclusion

Brassica oleracea is an abundantly available agriwaste material that is effectively utilized to eradicate two potentially damaging dyes: Congo red (anionic) and brilliant green (cationic) from waste water by applying batch sorption. Surface characterization and morphological studies by FTIR and SEM analysis provided that active uptake or removal of both the dye CR and BG is carried out by electrostatic interface by carboxylic as well as hydroxyl moieties present in adsorbent. Also, the interspaces present on sorbent surface expedited the uptake of dye molecules in the form of ions traveling towards its surface. These ions (dye) followed intraparticle as well as film diffusion mechanism to get attached on the surface of adsorbent (BO). Adsorption isotherms carried out also exhibit best fitting of the Langmuir isotherm model on the basis of R^2 being the highest among all used here along with q_{max} 42.553 and 103.093 for CR and BG, correspondingly. This clearly supports a homogenous monolayer adsorption of dyes CR and BG. Kinetic modeling gives its results in favor of Elovich and pseudosecond order model which shows that chemisorption occurs between the molecules of dye and adsorbent. Thermodynamic parameters (ΔG°, ΔH°, and ΔS°) studied also revealed that this process is appeared to be a spontaneous, exothermic process. Thus, all this proved that it is a physiochemical biosorption procedure highly effective for the removal of dyes from waste water, as summarized in Figure 8.

Abbreviations

FT-IR: Fourier-transform infrared spectroscopy
CR: Congo red dye
BG: Brilliant green dye
BO: *Brassica oleracea*
SEM: Scanning electron microscopy
PH_{pzc}: Point of zero charge.

Data Availability

All data related to this work is presented in Results along with references.

Conflicts of Interest

The authors declare that they have no conflicts of interest regarding the publications of this paper.

Acknowledgments

The authors are thankful to the home institute for providing facilities for this work.

References

[1] M. A. Hassaan, A. El Nemr, and A. Hassaan, "Health and environmental impacts of dyes: mini review," *American Journal of Environmental Science and Engineering*, vol. 1, no. 3, pp. 64–67, 2017.

[2] R. Gong, M. Li, C. Yang, Y. Sun, and J. Chen, "Removal of cationic dyes from aqueous solution by adsorption on peanut hull," *Journal of Hazardous Materials*, vol. 121, no. 1-3, pp. 247–250, 2005.

[3] E. Forgacs, T. Cserháti, and G. Oros, "Removal of synthetic dyes from wastewaters: a review," *Environment International*, vol. 30, no. 7, pp. 953–971, 2004.

[4] A. Dąbrowski, "Adsorption – from theory to practice," *Advances in Colloid and Interface Science*, vol. 93, no. 1-3, pp. 135–224, 2001.

[5] S. Gita, A. Hussan, and T. Choudhury, "Impact of textile dyes waste on aquatic environments and its treatment," *Environment and Ecology*, vol. 35, no. 3C, pp. 2349–2353, 2017.

[6] J. Mittal, V. Thakur, and A. Mittal, "Batch removal of hazardous azo dye Bismark Brown R using waste material hen feather," *Ecological Engineering*, vol. 60, pp. 249–253, 2013.

[7] R. A. E.-G. Mansour, M. G. Simeda, and A. A. Zaatout, "Removal of brilliant green dye from synthetic wastewater under batch mode using chemically activated date pit carbon," *RSC Advances*, vol. 11, no. 14, pp. 7851–7861, 2021.

[8] R. Rehman, S. J. Muhammad, and M. Arshad, "Brilliant green and acid orange 74 dyes removal from water by Pinus roxburghii leaves in naturally benign way: an application of green chemistry," *Journal of Chemistry*, vol. 2019, Article ID 3573704, 10 pages, 2019.

[9] R. D. Saini, "Textile organic dyes: polluting effects and elimination methods from textile waste water," *Int J Chem Eng Res*, vol. 9, no. 1, pp. 121–136, 2017.

[10] V. Vimonses, S. Lei, B. Jin, C. W. K. Chow, and C. Saint, "Adsorption of Congo red by three Australian kaolins," *Applied Clay Science*, vol. 43, no. 3-4, pp. 465–472, 2009.

[11] S. Haq, A. W. Raja, S. U. Rehman et al., "Phytogenic synthesis and characterization of NiO-ZnO nanocomposite for the photodegradation of brilliant green and 4-nitrophenol," *Journal of Chemistry*, vol. 2021, Article ID 3475036, 10 pages, 2021.

[12] M. Toor, B. Jin, S. Dai, and V. Vimonses, "Activating natural bentonite as a cost-effective adsorbent for removal of Congo-red in wastewater," *Journal of Industrial and Engineering Chemistry*, vol. 21, pp. 653–661, 2015.

[13] A. Srinivasan and T. Viraraghavan, "Decolorization of dye wastewaters by biosorbents: a review," *Journal of Environmental Management*, vol. 91, no. 10, pp. 1915–1929, 2010.

[14] V. Gomez, M. Larrechi, and M. Callao, "Kinetic and adsorption study of acid dye removal using activated carbon," *Chemosphere*, vol. 69, no. 7, pp. 1151–1158, 2007.

[15] M. T. Yagub, T. K. Sen, S. Afroze, and H. M. Ang, "Dye and its removal from aqueous solution by adsorption: a review," *Advances in Colloid and Interface Science*, vol. 209, pp. 172–184, 2014.

[16] R. Dutta, T. V. Nagarjuna, S. A. Mandavgane, and J. D. Ekhe, "Ultrafast removal of cationic dye using agrowaste-derived mesoporous adsorbent," *Industrial & Engineering Chemistry Research*, vol. 53, no. 48, pp. 18558–18567, 2014.

[17] J. Igwe and A. Abia, "A bioseparation process for removing heavy metals from waste water using biosorbents," *African Journal of Biotechnology*, vol. 5, no. 11, 2006.

[18] H. Freundlich, "Über die adsorption in lösungen," *Zeitschrift für Physikalische Chemie*, vol. 57U, no. 1, pp. 385–470, 1907.

[19] A. K. Kushwaha, N. Gupta, and M. Chattopadhyaya, "Removal of cationic methylene blue and malachite green dyes from aqueous solution by waste materials of _Daucus carota_," *Journal of Saudi Chemical Society*, vol. 18, no. 3, pp. 200–207, 2014.

[20] V. S. Mane, I. D. Mall, and V. C. Srivastava, "Kinetic and equilibrium isotherm studies for the adsorptive removal of brilliant green dye from aqueous solution by rice husk ash," *Journal of Environmental Management*, vol. 84, no. 4, pp. 390–400, 2007.

[21] A. Khaled, A. E. Nemr, A. el-Sikaily, and O. Abdelwahab, "Removal of direct N Blue-106 from artificial textile dye effluent using activated carbon from orange peel: adsorption isotherm and kinetic studies," *Journal of Hazardous Materials*, vol. 165, no. 1-3, pp. 100–110, 2009.

[22] N. Kannan and R. Pagutharivalan, "A comparative adsorption study with different activated carbons as adsorbents for the removal of cationic dye from aqueous solution," *Journal of Applicable Chemistry*, vol. 1, no. 1, pp. 22–38, 2012.

[23] B. Cojocariu, A. M. Mocanu, G. Nacu, and L. Bulgariu, "Possible utilization of PET waste as adsorbent for Orange G dye removal from aqueous media," *Desalination and Water Treatment*, vol. 104, pp. 338–345, 2018.

[24] L. Bulgariu, L. B. Escudero, O. S. Bello et al., "The utilization of leaf-based adsorbents for dyes removal: a review," *Journal of Molecular Liquids*, vol. 276, pp. 728–747, 2019.

[25] A. A. Yaseen and S. J. Ahmed, "Interaction effect of planting date and foliar application on some vegetative growth characters and yield of broccoli (brassica olerasea var italica) grown under unheated plastic tunnel," *J. of Gramian. University. ICBS Conference, Erbil.*, vol. 4, pp. 405–418, 2017.

[26] B. Grout, *Cauliflower (Brassica oleracea var. botrytis L.), in Crops II1988*, Springer, 1988.

[27] C. Beecher, "Cancer preventive properties of varieties of Brassica oleracea: a review," *The American Journal of Clinical Nutrition*, vol. 59, no. 5, pp. 1166S–1170S, 1994.

[28] P. Saravanan, J. Josephraj, B. P. Thillainayagam, and G. Ravindiran, "Evaluation of the adsorptive removal of cationic dyes by greening biochar derived from agricultural biowaste of rice husk," *Biomass Conversion and Biorefinery*, pp. 1–14, 2021.

[29] J. Borowski, A. Szajdek, E. J. Borowska, E. Ciska, and H. Zieliński, "Content of selected bioactive components and antioxidant properties of broccoli (Brassica oleracea L.)," *European Food Research and Technology*, vol. 226, no. 3, pp. 459–465, 2008.

[30] S. Ansar, H. Tabassum, N. S. Aladwan et al., "Eco friendly silver nanoparticles synthesis by Brassica oleracea and its

antibacterial, anticancer and antioxidant properties," *Scientific Reports*, vol. 10, no. 1, pp. 1–12, 2020.

[31] A. H. Jawad, A. S. Waheeb, R. Abd Rashid, W. I. Nawawi, and E. Yousif, "Equilibrium isotherms, kinetics, and thermodynamics studies of methylene blue adsorption on pomegranate (Punica granatum) peels as a natural low-cost biosorbent," *Desalination and Water Treatment*, vol. 105, pp. 322–331, 2018.

[32] R. C. Pundlik, S. D. Chowdhury, R. R. Dash, and P. Bhunia, "Life-Cycle Assessment of Agricultural Waste-Based and Biomass-Based Adsorbents," *Biomass, Biofuels, Biochemicals*, pp. 669–695, 2021.

[33] S. Latif, R. Rehman, M. Imran, S. Iqbal, A. Kanwal, and L. Mitu, "Removal of acidic dyes from aqueous media usingCitrullus lanatuspeels: an agrowaste-based adsorbent for environmental safety," *Journal of Chemistry*, vol. 2019, Article ID 6704953, 9 pages, 2019.

[34] R. Rehman, B. Salariya, and L. Mitu, "Batch scale adsorptive removal of brilliant green dye using Trapa natans peels in cost effective manner," *Revue Chimique*, vol. 67, pp. 1333–1337, 2016.

[35] M. A. M. Salleh, D. K. Mahmoud, W. A. W. A. Karim, and A. Idris, "Cationic and anionic dye adsorption by agricultural solid wastes: a comprehensive review," *Desalination*, vol. 280, no. 1-3, pp. 1–13, 2011.

[36] L. Radovic, I. F. Silva, J. I. Ume, J. A. Menéndez, C. A. L. Y. Leon, and A. W. Scaroni, "An experimental and theoretical study of the adsorption of aromatics possessing electron-withdrawing and electron-donating functional groups by chemically modified activated carbons," *Carbon*, vol. 35, no. 9, pp. 1339–1348, 1997.

[37] D. Savova, N. Petrov, M. F. Yardim et al., "The influence of the texture and surface properties of carbon adsorbents obtained from biomass products on the adsorption of manganese ions from aqueous solution," *Carbon*, vol. 41, no. 10, pp. 1897–1903, 2003.

[38] L. Zhu, C. Guan, B. Zhou et al., "Adsorption of dyes onto sodium alginate graft poly (acrylic acid-co-2-acrylamide-2-methyl propane sulfonic acid)/kaolin hydrogel composite," *Polymers and Polymer Composites*, vol. 25, no. 8, pp. 627–634, 2017.

[39] B. Acemioğlu, "Adsorption of Congo red from aqueous solution onto calcium-rich fly ash," *Journal of Colloid and Interface Science*, vol. 274, no. 2, pp. 371–379, 2004.

[40] N. Tripathi, "Cationic and anionic dye adsorption by agricultural solid wastes: a comprehensive review," *Journal of Applied Chemistry*, vol. 5, 108 pages, 2013.

[41] K. S. Baidya and U. Kumar, "Adsorption of brilliant green dye from aqueous solution onto chemically modified areca nut husk," *South African Journal of Chemical Engineering*, vol. 35, pp. 33–43, 2021.

[42] S. Wang, Y. Boyjoo, A. Choueib, and Z. H. Zhu, "Removal of dyes from aqueous solution using fly ash and red mud," *Water Research*, vol. 39, no. 1, pp. 129–138, 2005.

[43] I. Langmuir, "The adsorption of gases on plane surfaces of glass, mica and platinum," *Journal of the American Chemical Society*, vol. 40, no. 9, pp. 1361–1403, 1918.

[44] J. N. Wekoye, W. C. Wanyonyi, P. T. Wangila, and M. K. Tonui, "Kinetic and equilibrium studies of Congo red dye adsorption on cabbage waste powder," *Environmental Chemistry and Ecotoxicology*, vol. 2, pp. 24–31, 2020.

[45] A. L. Vega-Negron, L. Alamo-Nole, O. Perales-Perez, A. M. Gonzalez-Mederos, C. Jusino-Olivencia, and F. R. Roman-Velazquez, "Simultaneous adsorption of cationic and anionic dyes by chitosan/cellulose beads for wastewaters treatment," *International Journal of Environmental Research*, vol. 12, no. 1, pp. 59–65, 2018.

[46] S. Basharat, R. Rehman, T. Mahmud, S. Basharat, and L. Mitu, "Tartaric acid-modified Holarrhena antidysenterica and Citrullus colocynthis biowaste for efficient eradication of crystal violet dye from water," *Journal of Chemistry*, vol. 2020, Article ID 8862167, 18 pages, 2020.

[47] H. Freundlich, "Over the adsorption in solution," *The Journal of Physical Chemistry*, vol. 57, no. 385471, pp. 1100–1107, 1906.

[48] A. Mittal, J. Mittal, A. Malviya, and V. K. Gupta, "Removal and recovery of Chrysoidine Y from aqueous solutions by waste materials," *Journal of Colloid and Interface Science*, vol. 344, no. 2, pp. 497–507, 2010.

[49] J. O. Eniola, R. Kumar, A. A. al-Rashdi, M. O. Ansari, and M. A. Barakat, "Fabrication of novel Al (OH) 3/CuMnAl-layered double hydroxide for detoxification of organic contaminants from aqueous solution," *ACS Omega*, vol. 4, no. 19, pp. 18268–18278, 2019.

[50] D. Ringot, B. Lerzy, K. Chaplain, J. P. Bonhoure, E. Auclair, and Y. Larondelle, "In vitro biosorption of ochratoxin A on the yeast industry by-products: Comparison of isotherm models," *Bioresource Technology*, vol. 98, no. 9, pp. 1812–1821, 2007.

[51] M. R. Samarghandi, M. Hadi, S. Moayedi, and A. F. Barjesteh, *Two-Parameter Isotherms of Methyl Orange Sorption by Pinecone Derived Activated Carbon*, 2009.

[52] M. H. Jnr and A. I. Spiff, "Equilibrium sorption study of Al3+, Co2+ and ag+ in aqueous solutions by fluted pumpkin (Telfairia occidentalis HOOK f) waste biomass," *Acta Chimica Slovenica*, vol. 52, pp. 174–181, 2005.

[53] C. Namasivayam and D. Kavitha, "Removal of Congo red from water by adsorption onto activated carbon prepared from coir pith, an agricultural solid waste," *Dyes and Pigments*, vol. 54, no. 1, pp. 47–58, 2002.

[54] Z. Hu, H. Chen, F. Ji, and S. Yuan, "Removal of Congo red from aqueous solution by cattail root," *Journal of Hazardous Materials*, vol. 173, no. 1-3, pp. 292–297, 2010.

[55] R. Han, D. Ding, Y. Xu et al., "Use of rice husk for the adsorption of Congo red from aqueous solution in column mode," *Bioresource Technology*, vol. 99, no. 8, pp. 2938–2946, 2008.

[56] G. Annadurai, R.-S. Juang, and D.-J. Lee, "Use of cellulose-based wastes for adsorption of dyes from aqueous solutions," *Journal of Hazardous Materials*, vol. 92, no. 3, pp. 263–274, 2002.

[57] M. Foroughi-dahr, H. Abolghasemi, M. Esmaieli, G. Nazari, and B. Rasem, "Experimental study on the adsorptive behavior of Congo red in cationic surfactant-modified tea waste," *Process Safety and Environmental Protection*, vol. 95, pp. 226–236, 2015.

[58] G. C. Panda, S. K. Das, and A. K. Guha, "Jute stick powder as a potential biomass for the removal of Congo red and rhodamine B from their aqueous solution," *Journal of Hazardous Materials*, vol. 164, no. 1, pp. 374–379, 2009.

[59] R. Ahmad and R. Kumar, "Adsorptive removal of Congo red dye from aqueous solution using bael shell carbon," *Applied Surface Science*, vol. 257, no. 5, pp. 1628–1633, 2010.

[60] N. Kannan and M. Meenakshisundaram, "Adsorption of Congo red on various activated carbons. A comparative study," *Water, Air, and Soil Pollution*, vol. 138, no. 1/4, pp. 289–305, 2002.

[61] A. R. Abdul Rahim, H. M. Mohsin, K. B. L. Chin, K. Johari, and N. Saman, "Promising low-cost adsorbent from desiccated coconut waste for removal of Congo red dye from aqueous solution," *Water, Air, & Soil Pollution*, vol. 232, no. 9, pp. 1–11, 2021.

[62] D. Zewde and B. Geremew, "Removal of Congo red usingVernonia amygdalinaleaf powder: optimization, isotherms, kinetics, and thermodynamics studies," *Environmental Pollutants and Bioavailability*, vol. 34, no. 1, pp. 88–101, 2022.

[63] S. M. Badr and S. Isra'a, "Using agricultural waste as biosorbent for hazardous brilliant green dye removal from aqueous solutions," *Journal of Engineering Science and Technology*, vol. 16, no. 4, pp. 3435–3454, 2021.

[64] R. Atef, N. Aboeleneen, and N. M. AbdelMonem, "Preparation and characterization of low-cost nano-particle material usingpomegranate peelsfor brilliant green removal," *International Journal of Phytoremediation*, pp. 1–11, 2022.

[65] M. S. Hussain, R. Rehman, and M. Imran, "Comparative evaluation of the adsorption performance of citric acid-treated peels of Trapa natans and Citrullus lanatus for cationic dyes degradation from water," *Journal of Chemistry*, vol. 2022, Article ID 1109376, 19 pages, 2022.

[66] S. Basharat, R. Rehman, and L. Mitu, "Adsorptive separation of brilliant green dye from water by tartaric acid-treated holarrhena antidysenterica and Citrullus colocynthis biowaste," *Journal of Chemistry*, vol. 2021, Article ID 6636181, 18 pages, 2021.

[67] P. Samiyammal, A. Kokila, L. A. Pragasan et al., "Adsorption of brilliant green dye onto activated carbon prepared from cashew nut shell by KOH activation: studies on equilibrium isotherm," *Environmental Research*, vol. 212, article 113497, 2022.

[68] G. Vyavahare, R. Gurav, R. Patil et al., "Sorption of brilliant green dye using soybean straw-derived biochar: characterization, kinetics, thermodynamics and toxicity studies," *Environmental Geochemistry and Health*, vol. 43, no. 8, pp. 2913–2926, 2021.

[69] C. Theivarasu and S. Mylsamy, "Equilibrium and kinetic adsorption studies of rhodamine-B from aqueous solutions using cocoa (Theobroma cacao) shell as a new adsorbent," *International Journal of Engineering, Science and Technology*, vol. 2, no. 11, pp. 6284–6292, 2010.

[70] N. Ayawei, J. Godwin, and D. Wankasi, "Synthesis and sorption studies of the degradation of Congo red by Ni-Fe layered double hydroxide," *International Journal of Applied Chemical Sciences Research*, vol. 13, no. 3, pp. 1197–1217, 2015.

[71] O. A. Habeeb, K. Ramesh, G. A. M. Ali, R. M. Yunus, and O. A. Olalere, "Kinetic, isotherm and equilibrium study of adsorption capacity of hydrogen sulfide-wastewater system using modified eggshells," *IIUM Engineering Journal*, vol. 18, no. 1, pp. 13–25, 2017.

[72] S. M. Al-Garni, "Biosorption of lead by gram-ve capsulated and non-capsulated bacteria," *Water SA*, vol. 31, no. 3, pp. 345–350, 2005.

[73] M. Gubernak, W. Zapala, and K. Kaczmarski, "Analysis of amylbenzene adsorption equilibria on an RP-18e chromatographic column," *Acta Chromatographica*, pp. 38–59, 2003.

[74] O. Hamdaoui and E. Naffrechoux, "Modeling of adsorption isotherms of phenol and chlorophenols onto granular activated carbon: part I. two-parameter models and equations allowing determination of thermodynamic parameters," *Journal of Hazardous Materials*, vol. 147, no. 1-2, pp. 381–394, 2007.

[75] A. Achmad, J. Kassim, T. K. Suan, R. C. Amat, and T. L. Seey, "Equilibrium, kinetic and thermodynamic studies on the adsorption of direct dye onto a novel green adsorbent developed from Uncaria gambir extract," *Journal of Physical Science*, vol. 23, no. 1, pp. 1–13, 2012.

[76] W. Zhu, J. Liu, and M. Li, "Fundamental studies of novel zwitterionic hybrid membranes: kinetic model and mechanism insights into strontium removal," *The Scientific World Journal*, vol. 2014, Article ID 485820, 7 pages, 2014.

[77] Y.-S. Ho and G. McKay, "Sorption of dye from aqueous solution by peat," *Chemical Engineering Journal*, vol. 70, no. 2, pp. 115–124, 1998.

[78] K. D. Kowanga, E. Gatebe, G. O. Mauti, and E. M. Mauti, "Kinetic, sorption isotherms, pseudo-first-order model and pseudo-second-order model studies of cu (II) and Pb (II) using defatted Moringa oleifera seed powder," *The Journal of Phytopharmacology*, vol. 5, no. 2, pp. 71–78, 2016.

[79] S. Chawla, H. Uppal, M. Yadav, N. Bahadur, and N. Singh, "Zinc peroxide nanomaterial as an adsorbent for removal of Congo red dye from waste water," *Ecotoxicology and Environmental Safety*, vol. 135, pp. 68–74, 2017.

[80] C. Tang, Y. Zhang, J. Han, Z. Tian, L. Chen, and J. Chen, "Monitoring graphene oxide's efficiency for removing Re(VII) and Cr(VI) with fluorescent silica hydrogels," *Environmental Pollution*, vol. 262, article 114246, 2020.

[81] Q. Zhu, G. D. Moggridge, and C. D'Agostino, "Adsorption of pyridine from aqueous solutions by polymeric adsorbents MN 200 and MN 500. Part 2: kinetics and diffusion analysis," *Chemical Engineering Journal*, vol. 306, pp. 1223–1233, 2016.